Published in final edited form as:
*Vis Neurosci*. 2009 ; 26(2): 215–226. doi:10.1017/S0952523809090063.

# Distribution and structure of efferent synapses in the chicken retina

**SH Lindstrom**[1], **N Nacsa**[2], **T Blankenship**[3], **PG Fitzgerald**[3], **C Weller**[1], **DI Vaney**[2], and **M Wilson**[1]

[1]Department of Neurobiology, Physiology and Behavior, Division of Biological Sciences, University of California, Davis, California, 95616 USA

[2]ARC Centre of Excellence in Vision Science, Queensland Brain Institute, University of Queensland, Brisbane, Queensland 4072

[3]Department of Cell Biology and Human Anatomy, School of Medicine, University of California, Davis, California, 95616 USA

## Abstract

The visual system of birds includes an efferent projection from a visual area, the isthmooptic nucleus in the midbrain, back to the retina. Using a combination of anterograde labeling of efferent fibers, reconstruction of dye-filled neurons, NADPH-diaphorase staining, and transmission electron microscopy we have examined the distribution of efferent fibers and their synaptic structures in the chicken retina. We show that efferent fibers terminate strictly within the ventral retina. In 2 completely mapped retinas, only 2 fibers from a total of 15,359 terminated in the dorsal retina. The major synapse made by each efferent fiber is with a single Efferent Target Amacrine Cell (TC). This synapse consists of 5-25 boutons of 2μm diameter, each with multiple active zones, pressed into the TC soma or synapsing with a basketwork of rudimentary TC dendrites in the inner nuclear layer (INL). This basketwork, which is sheathed by Muller cells processes, defines a private neuropil in the INL within which TCs were also seen to receive input from retinal neurons. In addition to the major synapse, efferent fibers typically produce several very thin processes that terminate nearby in single small boutons and for which the soma of a local amacrine cell is one of the likely postsynaptic partners. A minority of efferent fibers also give rise to a thicker process terminating in a strongly diaphorase positive ball about 5μm in diameter.

### Keywords

amacrine cell; Isthmo-optic nucleus; avian; retinopetal; centrifugal visual system

## Introduction

The visual system of birds includes a substantial projection from the brain to the retina. The major part of this efferent input, also known as a centrifugal or retinopetal input, originates from the contralateral isthmo-optic nucleus (ION), a visual nucleus found at the dorsal surface of the midbrain. The function of this centrifugal visual system (CVS) is unknown but a number of anatomical and physiological results imply that it works rapidly to enhance local retinal responses (Holden & Powell, 1972; Li *et al.*, 1998; Uchiyama *et al.*, 1998). Although there have been numerous anatomical studies of the efferent system within the

**Corresponding author:** Martin Wilson Department of Neurobiology, Physiology and Behavior, Division of Biological Sciences, University of California, Davis, California, 95616 USA Phone: (530) 752-7250; Fax: (530) 752-5582; mcwilson@ucdavis.edu.

retina since its original description in the late 19th century, several questions pertinent to its function presently have no clear answer. In this study we reexamine, in detail, the anatomy of efferent input to a bird retina.

In ground feeding birds, where the ION is most prominent, approximately 8,500 myelinated efferent fibers, so called restricted efferent fibers (rEFs) (Ramón y Cajal, 1889; Fritzsch *et al.*, 1990; Nickla *et al.*, 1994), run to each retina (Cowan & Powell, 1962). In the chicken retina (Catsicas *et al.*, 1987b; Fritzsch *et al.*, 1990; Cellerino *et al.*, 2000), and that of the quail (Uchiyama & Stell, 2005), efferent input is reported to be concentrated in the inferior retina, but only in the pigeon is a density map available (Hayes & Holden, 1983). Even in this species, however, it is unclear how strict is the exclusion from the dorsal retina since sampled densities of less than 50 $mm^{-2}$ were scored as zero. By mapping the position of every rEF terminal we show here that this rule is very strict, unexpectedly so in view of the prevailing notion that the retinal position of efferent terminals is immaterial to their function (Uchiyama & Stell, 2005).

Within the retina, of Galliform birds at least, every rEF is thought to make synaptic contact with a single amacrine cell (Uchiyama & Ito, 1993; Uchiyama *et al.*, 1995). Both the synapse and the amacrine cell are unusual. The amacrine cell, often called the efferent target cell or simply target cell (TC), has a large prolate soma located in the inner and middle region of the inner nuclear layer (INL). The basal portion of the soma gives rise to a few rudimentary (<5 μm length) dendrites and one axon that runs for 0.5-6 mm along the border of the INL and inner plexiform layer (IPL), before terminating in stratum 1 of the IPL (Ramón y Cajal, 1995; Uchiyama *et al.*, 2004). The absence of proper dendrites and the presence of an axon has prompted the suggestion that these cells should not be classified as amacrine cells but rather should have their own class (Uchiyama & Stell, 2005).

The synapse between rEFs and TCs is typically a large and complex structure in which an efferent terminal apparently surrounds the basal portion of the TC, in what Cajal termed a “pericellular nest” (Ramón y Cajal, 1889) and what has elsewhere been called a calyx-like synapse (Uchiyama & Stell, 2005). The two ultrastructural studies of this synapse both show numerous synaptic vesicles and many mitochondria in efferent terminals (Dowling & Cowan, 1966; Uchiyama & Ito, 1993) but differ in some important regards. In particular the more extensive study in the pigeon suggests that the pericellular nest around a TC is comparatively rare and the majority of efferent synapses are small basal contacts with “ordinary” amacrine cells (Dowling & Cowan, 1966). Because it bears on the possible function of the efferent system, an important but unresolved question is whether TCs are driven exclusively by their efferent input or whether a retinal input might also be present. In this study we use several anatomical methods to clarify the structure of both the pre and postsynaptic elements at this synapse in the chicken retina. We show that although TCs have only the shortest of dendrites, these receive input from other neurons in addition to rEFs in a “private” neuropil within the INL. As well as the major synapse every rEF makes with a TC, there are two other types of synapse formed by rEFs, one of which appears to be quite novel.

## Materials and Methods

A total of 105 young white leghorn chickens (*Gallus gallus*) were used in this study. Of these, 57 were hatched from eggs obtained from the Avian Sciences Facility of the University of California, Davis and used in surgeries to label the efferent fibers as described below. The experimental procedures were approved by the Institutional Animal Care and Use Committee at the University of California, Davis. The NADPH-diaphorase histochemistry portion of this study used 48, 3-week old, chickens from the University of

Queensland Central Animal House. The handling of these chickens was in accord with the Australian code of practice for the care and use of animals for scientific purposes.

Prior to surgeries intended to label efferent fibers, a set of preliminary experiments was performed to determine the typical position of the left isthmo-optic nucleus (ION) relative to the major cranial sutures. The location of the ION was revealed with retrograde labeling with Alexa 488 or 555 conjugated cholera toxin subunit B (Invitrogen, C-22841 & C-22842) injected into each eye, red in the right eye and green in the left (Fig. 1A&B). The position of the ION relative to the intersections of the major cranial sutures was then measured in three preserved chicken heads mounted in a custom stereotaxic frame.

### Labeling of efferent fibers

Two-week-old chickens were anesthetized with 1-3% isoflurane and mounted in the stereotaxic frame such that the dorsal surface of the skull was roughly horizontal. A sharp Hamilton syringe was then advanced, through a small hole drilled in the skull, to the estimated coordinates of the ION. 0.5 μL of the anatomical tracer, 15% Fluoro-Ruby (Invitrogen, D1817) or 10% Fluoro-Ruby with 10% Alexa 568 conjugated dextran (Invitrogen, D22912), in sterile saline, was injected over a 1 min period. The syringe was left in place for a minimum of 2 min before being removed. After sealing the skull with bone wax and closing the incision with sutures, the chicken was removed from anesthesia.

### Tissue preparation for fluorescence immunohistochemistry

Following a minimum survival period of 3 days, the chicken was euthanized with a lethal dose of pentobarbital (Beuthanasia-D, Webster Veterinary, 047305). Once the animal was deeply anesthetized, as assessed by a lack of the toe pinch reflex, it was transcardially perfused with phosphate buffered saline (PBS; Sigma) followed by 4% paraformaldehyde (PFA; Sigma) in PBS. The right eye was removed and hemisected just posterior to the ora serata. The posterior eyecup was postfixed in chilled 4% paraformaldehyde for 1-2 hrs. The brain was removed and postfixed overnight in chilled 4% paraformaldehyde.

The day after perfusion the brain was rinsed with PBS, embedded in 5% agar (Sigma, A9915), and sectioned at 50 μm thickness on a Vibratome. Transverse sections cut through the region of the midbrain containing the ION were transferred to slides, counterstained with SYBR-green (Invitrogen, S7564), and coverslipped with VectaShield hard-set mounting medium (Vector Labs, H1400). All sections containing portions of the ION were imaged to determine the extent to which the IO-neurons had taken up the tracer.

To prepare flat mounts, the eyecup was rinsed with PBS and cut in half with a single dorsal-ventral cut just temporal to the pecten. The pecten was carefully excised, to assure minimum loss of retina. The retina was removed from the sclera and pigment epithelium before being processed using standard immunohistochemistry techniques. The retinas used for the flat mount studies, in which we mapped the distribution of rEF terminals, came only from animals in which all of the IO-neurons had taken up tracer, as verified by inspecting sections drawn from the entire extent of the ION.

To prepare radial sections of the retina, the eyecup was rinsed with PBS and two 5 mm × 5 mm squares, corresponding to the regions of the retina where efferent fibers are found in highest density, were cut out from either side of the pecten. These retinal squares were separated from the sclera and placed in 30% sucrose solution at 4°C until equilibrated (typically overnight). The following day they were embedded in OCT medium (Ted Pella, 27050), frozen on dry ice, and stored at −20°C until sectioning. Sections of 12-20 μm were cut on a cryostat (Leica CM1900), mounted on gelatin coated slides, and stored at −20°C.

### Fluorescence immunohistochemistry

To identify TCs we used the same anti-parvalbumin antibody used by Fischer and Stell (1999) for this purpose (Fig. 1C). For flat mounts labeled with both Fluoro-Ruby and anti-parvalbumin, a blocking solution containing 10% normal goat serum, 1% BSA, and 0.1% Tween-20 in PBS was applied for 1 hr at room temperature. Retinas were incubated in mouse anti-parvalbumin (Sigma, P3088) diluted 1:1000 in blocking solution for 7 days at 4°C, washed 3x in PBS (40, 20, 20 min), then incubated for 1-5 days at 4°C in secondary antibodies (Alexa 568-conjugated goat anti-mouse; Invitrogen) diluted 1:500 in PBS. Finally, the flat mounts were washed with PBS and coverslipped using VectaShield hard-set mounting medium (Vector Labs, H1400). The following day the slides were sealed using DPX (Fischer, NC 9753710).

Retinal sections were processed for immunohistochemistry using techniques similar to those described for flat mounts, except that sections were quenched with 1% glycine in 0.3% Triton-PBS for 15 min prior to blocking solution, and the incubation times for primary and secondary antibodies were reduced to overnight and 1-2 hrs, respectively.

Stained sections and flat mounts were examined using an inverted confocal microscope (Olympus FLUOVIEW) employing krypton (488 nm) and argon (568 nm) lasers. Images were converted to 24-bit TIF images in Fluoview software then transferred to Adobe Photoshop for adjustment of brightness, contrast and sharpness. Images of antibody labeled tissue were always processed identically to images of the corresponding secondary-only control. These are not shown, because they were uniformly black.

### Construction of rEF density maps

Confocal images were acquired for the entire extent of two retinal flat mounts (roughly 200 images per retina). Compressed z-stacks of the INL-IPL border were montaged in Adobe Photoshop, and loaded into Neurolucida to allow mapping of the locations of every Fluoro-Ruby labeled rEF. Neurolucida maps representing every rEF terminal as a point were then converted to density maps by convolution with a 2-dimensional Gaussian function implemented in MathCad.

### Filling TCs with Lucifer yellow

Some TCs, identified as such by the presynaptic labeling of an rEF with Fluoro-Ruby, were injected with Lucifer yellow in flat mount retinas lightly fixed in 4% PFA in PBS for 20 min on ice. For these experiments, both nasal and temporal pieces of retina were attached to black Millipore papers (Millipore AABG02500; Millipore, Bedford, MA) prior to fixation. The tips of injection micropipettes were filled with 2% Lucifer yellow (Sigma) in 0.1 M Tris buffer, pH 8.2. Lucifer yellow was iontophoresed with −1 nA current for 60 sec, and cells were then left to equilibrate for 30 min in Ames medium (Sigma, St. Louis, MO) containing 1.9 g/liter of $NaHCO_3$ (pH 7.4 at room temperature) and adjusted to 320mOsmol with NaCl, before a second fixation in 4% PFA in 0.1M PBS for 30 minutes. Following an overnight wash in PBS with 0.2% Triton, retinas were blocked with 3% Donkey Serum in PBS for one day, and incubated in anti-Lucifer yellow antibody (Polyclonal Rabbit anti-Lucifer yellow; Invitrogen, A-5750) diluted 1:10,000 in 1% Donkey serum in PBS for approximately 5 days. Retinas were washed in PBS with 0.2% Triton overnight, then incubated in secondary antibody (Cy2-conjugated AffiniPure Donkey Anti-Rabbit IgG (H+L); Jackson ImmunoResearch, 711-225-152) diluted 1:200 in 1% Donkey serum in PBS for approximately 24 hrs. Retinas were washed overnight in 0.1M PBS then subsequently mounted in Prolong Gold antifade solution (Invitrogen, P36934).

### Tissue preparation for NADPH-diaphorase histochemistry

Retina from the nasal, and temporal halves of the eyecup was gently removed from the pigment epithelium and mounted photoreceptor side down, on black Millipore paper. Retinal halves were maintained, until processing, in carbogenated Ames medium. A two-step procedure was used in which NADPH was synthesized *in situ* by reduction of NADP using malic acid as the substrate for endogenous malic enzyme (Sagar, 1986; Vaney & Young, 1988; Vaney, 2004). Retinas were fixed with 4% PFA in 0.1 M PBS for 20 min at room temperature, followed by several washes and overnight in 0.2% Triton in 0.1 M Tris buffer (pH 8.2). Solutions used for the diaphorase reaction were as described in Vaney and Young (1988). The reaction was allowed to proceed for 90 minutes at 37°C and was then stopped by extensive washing in Tris buffered saline (pH 7.6). After retinas were removed from their Millipore filters they were coverslipped as flat mount preparations with 50% glycerol in PBS.

### Tissue preparation for electron microscopy

For tissue not treated with antibodies, eye cups were immediately placed in 4% glutaraldehyde and 2% PFA in PBS for 2+ hrs at 4°C. Fixed eye cups were thoroughly washed with PBS and cut into squares with high EF density prior to osmication. For those experiments using pre-embedding staining for parvalbumin we started with 300-500 μm thick slices cut from retinas lightly fixed in chilled 4% paraformaldehyde for 1hr. After blocking in 10% normal goat serum and PBS for 1hr, sections were incubated in the primary antibody, mouse anti-parvalbumin (Sigma, P3088), diluted 1:1000 in PBS with 1% sodium azide and 1% saponin (Sigma, 16109) for 5 d. Three 20-min washes in PBS both preceded and followed application of the secondary antibody, biotinylated goat anti-mouse (Vector Labs, Vectastain ABC kit, NC9275715), diluted 1:200 in PBS with 1% saponin and 1% sodium azide. Sections remained in the secondary antibody for 2d and were then incubated in a 1:50 dilution of an Avidin-Biotinylated horseradish peroxidase Complex (Vector Labs, Vectastain ABC kit, NC9275715) for 1hr, rinsed in PBS, and reacted in a solution of 0.05% 3,3′-diaminobenzidine (DAB; Sigma, D5637) and 0.1% hydrogen peroxide, with the addition of 0.025% cobalt chloride and 0.02% nickel ammonium sulfate for signal intensification (Adams, 1981; Vugler et al., 2008). The reaction was allowed to proceed for approximately 45min with frequent solution replacement. Thorough washing in PBS terminated the reaction, and the sections were postfixed with 0.1% glutaraldehyde for 1hr rinsed in PBS prior to osmication. For all EM material, small pieces of retina from the high EF density region were postfixed in 1% osmium tetroxide in 0.1 M phosphate buffer (pH 7.3) for one hour. After buffer rinses, the retinal pieces were dehydrated in a graded series of ethanol, incubated in propylene oxide, then infiltrated and embedded with epoxy resin (Poly/Bed 812; Polysciences Inc.). Thick sections of the retinas were obtained for initial examination, and then thin sections were cut from selected areas. Thin sections were stained with uranyl acetate and lead citrate prior to examination with a Philips CM120 transmission electron microscope.

## Results

### Anterograde labeling of rEFs and identification of TCs

Injection of Fluoro-Ruby into the ION produced fluorescent labeling that was visible 3 days later in the contralateral retina. In whole mount preparations, fibers in which the label had been anterogradely transported were seen to exit the optic nerve head, fan out in the fiber layer before diving into the IPL. Two distinct kinds of fiber were recognizable. The more numerous rEFs could be recognized as thick fibers, without collaterals, that swelled into dense synaptic terminals at the INL-IPL border (asterisks in Fig. 2 & Fig. 3A panel c). In confocal cross-section each rEF was seen to form a donut of Fluoro-Ruby filled terminals

around the soma of a single TC (arrowheads in Fig. 3A panels a & b). In addition to the rEFs, thin fibers with a beaded appearance and multiple collaterals (arrows in Fig. 2) could also be seen. These are the "widespread efferent fibers" (wEFs) originating from a halo of "ectopic neurons" lying just outside the ION (Dogiel, 1895; Hayes & Webster, 1981; Chmielewski *et al.*, 1988; Fritzsch *et al.*, 1990) and whose anatomy we have not investigated further.

### Density map of the rEF terminals

To enable ultrastructural examination of rEF terminals it was necessary first to find the retinal locations in which terminal density was highest. In addition to this practical matter, the distribution of terminals is clearly a major constraint on theories of CVS function and justifies close examination. While older studies are ambiguous (Maturana & Frenk, 1965; McGill *et al.*, 1966; Crossland & Hughes, 1978), several more recent studies conclude that efferent input is concentrated in the ventral retina (Hayes & Holden, 1983; Catsicas *et al.*, 1987b; Uchiyama & Ito, 1993; Uchiyama *et al.*, 1995; Woodson *et al.*, 1995; Cellerino *et al.*, 2000; Uchiyama *et al.*, 2004; Uchiyama & Stell, 2005).

We examined the distribution of rEF terminals in two flat mount retinas from chickens in which the unilateral injection of Fluoro-Ruby labeled all IO-neurons, verified by inspecting sections, like the one in Fig. 4, drawn from the entire extent of the ION. Confocal microscopy was used to acquire images of the INL-IPL border over the entire extent of the retina. Roughly 200 images from each retina were montaged in Adobe Photoshop, and loaded into Neurolucida to allow mapping of the locations of every Fluoro-Ruby labeled rEF terminal. While wEFs were observed in these retinas, they were not included in these maps. The total number of rEFs in each retina was 7,193 and 8,166; however, the actual number is probably higher in each by a few hundred because some rEFs were unavoidably removed when the pecten was excised. The Neurolucida maps were converted to density maps, like the one shown in Figure 4, by convolution with a 2-D Gaussian function. These maps show that rEFs are found in highest density in a band just below the horizontal midline (max. density of ~320/mm$^2$). Lower densities of rEFs were found throughout the rest of the ventral retina and in the extreme ventral retina densities of less than 10/mm$^2$ could be seen. In both retinas, the extreme ventral region of the temporal quadrant was noticeably emptier than that of the nasal quadrant. In the dorsal retina, however, rEFs were completely absent. The transition between the high rEF density band and the empty dorsal region was abrupt (declining from 320/mm$^2$ to 0/mm$^2$ in 1.5 mm) creating a clear boundary between the ventral and dorsal retina (dotted line in Fig. 4).

### One-to-one contacts between rEFs and TCs

A separate set of flat mounted retinas, from chickens in which the Fluoro-Ruby injection had resulted in complete labeling of the ION, were double labeled with an anti-parvalbumin antibody previously shown to identify 3 or 4 amacrine cell types (Sanna *et al.*, 1992). One of these types, the target cell (TC), is strongly positive and possesses a distinctly larger, flask-shaped soma extending higher in the inner nuclear layer than the others (Fischer & Stell, 1999). Confocal z-stacks were acquired from the upper IPL through to the top of TC somata in the INL. As shown in Figure 3B, each rEF contacts one and only one TC with a dense cluster of synaptic terminals that resembles the pericellular nest described by Cajal (1889; 1995), consistent with previous observations of the one-to-one connectivity in another Galliform bird (Uchiyama & Ito, 1993; Uchiyama *et al.*, 1995). Because we examined flat mounts in which TCs were labeled, we can add that we never observed a large, prolate, intensely parvalbumin-positive amacrine cell that was not surrounded by a Fluoro-Ruby labeled pericellular nest. Consistent with this, we found this type of cell to be absent from

the dorsal retina. We conclude that every TC receives input from one rEF and every rEF contacts one TC.

## NADPH-diaphorase histochemistry of the rEF terminal

Several studies have established that both rEFs and TCs are strongly NADPH-diaphorase positive (Morgan *et al.*, 1994; Goureau *et al.*, 1997; Fischer & Stell, 1999; Posada & Clarke, 1999; Rios *et al.*, 2000), reflecting the high levels of Nitric Oxide Synthase (NOS) expressed in these structures. We took advantage of this to examine the morphology of the rEF terminal in greater detail. A typical field of rEFs stained using the NADPH-diaphorase method is shown in Figure 5A. Also visible in this plane are TC axons, almost all of which run to the dorsal retina in the uppermost lamina of the IPL, as previously reported (Catsicas *et al.*, 1987a; Uchiyama *et al.*, 2004). As described for Fluoro-Ruby labeled retinas, the rEFs appear as thick fibers without collaterals that swell into a dense synaptic terminal, or pericellular nest (Figure 5A, large arrowheads). With this staining method it was possible to follow individual fibers from close to the optic nerve head to their eventual termination. Fibers run without branching and more or less straight in the fiber layer, until close to their termination where they dive through the ganglion cell layer and into the IPL. In the IPL a significant fraction of them split into 2 or more branches but invariably these branches converge, nevertheless, upon the same TC. The pericellular nest itself comprises 5-25, roughly spherical presynaptic structures, giving it the appearance of a bunch of grapes (see Fig. 5D). These grapes are ~2 μm in diameter and are typically distributed from the base of the TC soma to its equator.

In addition to the pericellular nest, the NADPH-diaphorase method reveals two other types of synaptic structure arising from the rEF. We have called these structures “tendrils” (long arrows in Fig. 5A) and the “ball and chain” (short arrows in Fig. 5A). A number of other diaphorase-positive cells can also be seen it this image; these are more fully described elsewhere (Wilson *et al*., in preparation). Tendrils and the ball and chain were not visible in Fluoro-Ruby labeled retinas, most likely because the tendrils and chain are too small to contain enough Fluoro-Ruby to be detected. This limitation is likely aggravated by the fact that Fluoro-Ruby is sequestered within intracellular organelles (Dacey *et al.*, 2003), rather than freely diffusable within the cytoplasm.

Tendrils are minute side branches (< 1 μm diameter) of the rEF terminal that end in a single, small (~ 0.7-1.5 μm) synaptic bouton usually no more than 10 μm from the pericellular nest. Most of the rEF terminals we examined with diaphorase staining gave rise to one or more tendrils. In Figure 5B, the large pericellular nest of a rEF (large arrowhead) is visible in the lower right, and a number of tendrils can be seen to branch off from portions of the pericellular nest. Most of these terminate in a synaptic bouton on an unknown target in the amacrine cell layer (small arrowheads) but, as was sometimes observed, one appears to contact a weakly diaphorase-positive amacrine cell soma (small arrow). This cell is found ubiquitously throughout the retina and is characterized by a monostratified dendritic field at an IPL depth of 80%. The density of these cells is highest around the horizontal meridian (1040/mm$^2$), high in the dorsal retina (800/mm$^2$) and about half that in the ventral retina. These neurons are undoubtedly those classified as type 1 by Fischer and Stell (1999) and are described in detail elsewhere (Wilson *et al*., in preparation).

Other authors have observed smaller processes that branch off the rEF pericellular nest and synapse with neighboring cells at the INL-IPL border (Ramón y Cajal, 1889; Ramón y Cajal, 1895; Maturana & Frenk, 1965; Chmielewski *et al.*, 1988; Fritzsch *et al.*, 1990). While detailed descriptions of the processes were not provided, we believe they are probably the tendrils we describe here. Maturana and Frenk (1965) and Hayes and Holden (1983) claimed that one of the targets of the tendril-like processes that they observed in pigeon was

a displaced ganglion cell (DGC). In our experiments, we did not see any evidence for tendril synapses with DGCs, which typically are weakly stained by NADPH-diaphorase. However, given that some DGCs were negative for NADPH-diaphorase we cannot eliminate the possibility that synapses between tendrils and these unstained DGCs were present but unobserved.

Like the tendrils, the ball and chain structure branches directly off the pericellular nest (see asterisk in Fig. 5C); however, the ball and chain is significantly larger and typically terminates further from the pericellular nest. The diameter of the chain is typically 1-2 μm and is often seen to have swollen regions. Unlike tendrils that rarely extend more than 10 μm from the pericellular nest, the ball and chain typically extends 20-30 μm. The ball itself is large, typically 5 μm in diameter and nearly spherical, with very intense staining for NADPH-diaphorase, suggesting that it expresses a high level of NOS. The postsynaptic partner(s) of this structure is (are) unknown, but they do not include TCs or any other diaphorase-positive neurons. Only a minority of rEF terminals gave rise to a ball and chain, and only very rarely was a single rEF seen with two. This synaptic structure has not been previously described.

## Morphology of the TC dendrites and initial segment

To visualize the structure of the TC we injected these cells with Lucifer yellow in lightly fixed retinas. Figure 6 shows a series of images from a confocal z-stack of one such cell. Images are referenced to the plane of the TC axon, just below the INL-IPL border (0 μm). The dendritic region spans the region 8.5 thru 14.5 μm and the soma extends upwards from about 12.5 μm though, in reality, there is no clear separation of these regions. The dendritic region tapers down into the initial segment of the TC axon which turns sharply to parallel the IPL-INL border in the uppermost layer of the IPL. The dendrites themselves are very short and anastomose to form an intricate basketwork confined to the INL and only rarely extending a little into the IPL. In the dendritic region there are several round holes approximately 2 μm in diameter, suggesting that the grapes of the rEF terminal fit into the dendritic basketwork surrounding the axon initial segment, but as seen in higher optical planes, grapes are also pressed into the soma, (arrows in Figure 6).

## Ultrastructure of the TC and neuropil

Using pieces of retina taken from the regions of highest rEF density we examined the ultrastructure of TCs in radial sections. In practice, we found that it was easily possible to identify TCs in electron micrographs based solely upon the pre- and postsynaptic features described in the previous sections. Specifically, we looked for large, prolate cells located in the inner third of the INL that were contacted by large, round synaptic terminals (the grapes of the rEF terminal). By these criteria, TCs were unambiguously identified and seen at a density consistent with Figure 4C, but as confirmation we visualized anti-parvalbumin binding using a heavy metal intensified HRP reaction method (Adams, 1981; Vugler *et al.*, 2008). Since primary antibody binding was eliminated by glutaraldehyde fixation we were obliged to use light fixation of the retina. Even though reduced fixation degraded the quality of EM images, it was nevertheless possible to see that cells we would otherwise classify as TCs contained heavy reaction product (data not shown).

As we inferred from the Lucifer yellow fills and diaphorase staining, there was marked variation between TCs in the placement of presynaptic grapes. In some (Figure 7A), grapes covered much of the soma whereas in others (Figure 7B), they were confined to the basal aspect of the cell. In all TCs, a striking feature of the rEF to TC synapse was that the zone of synaptic interaction between TC dendrites and the presynaptic rEF grapes was located above the IPL, within the INL (based on EM examination of 11 TCs). In addition, this zone of

synaptic interaction was curtained off from the surrounding amacrine cells by a sheath of Muller cell processes (the electron dense areas indicated by white arrowheads in Fig. 7B). Thus it appears that each TC receives synaptic input in its own "private neuropil" (dashed region in Fig. 7B), removed from the general region of interaction in the IPL. The volume of the private neuropil for the TC shown in Figure 7B we estimate to be roughly 500 $\mu m^3$.

At high magnification, EM images showed that rEF grapes, the presynaptic structures that form the pericellular nest, contain numerous mitochondria and an abundance of clear, round synaptic vesicles. Each presynaptic grape has multiple active zones characterized by pre and postsynaptic densities of approximately 300 nm diameter, around which a dense cloud of vesicles may be seen (Figure 8). The TC soma and its dendritic processes were characterized by a relatively dense cytoplasm containing clusters of ribosomes and rough endoplasmic reticulum. For the TC shown in Figure 9, processes that could be unambiguously identified as belonging to either the TC or the rEF on the basis of cytoplasmic appearance were colored green or red, respectively, while those processes that could not be unambiguously identified were left uncolored. Some of these ambiguous processes must belong to the TC or rEF, but others are apparently different, having very light cytoplasm and a low density of small, pleomorphic synaptic vesicles. One such process can be seen to make a synapse with one of the TC dendrites (circle in Fig. 9).

To confirm that these light-cytoplasm processes are genuinely different from the rEF terminals we compared the size of their synaptic vesicles by measuring the area of vesicles within these structures using ImageJ software. Measured area was then converted to equivalent diameter. The mean diameter of rEF vesicles was found to be 46 ± 15.1 nm whereas, for light-cytoplasm processes, the value was 37 ± 16.7 nm. A comparison of the distribution of vesicle sizes showed that these two populations of synaptic vesicles were significantly different ($p<0.001$; Kolmogorov-Smirnov Test). Pleomorphic synaptic vesicles are commonly a signature of GABAergic terminals elsewhere in the nervous system (Montero & Singer, 1984; Oberdorfer *et al.*, 1988; Mize *et al.*, 1994; Iliakis *et al.*, 1996; Hoshino *et al.*, 2000; Sherman & Guillery, 2002) and GABA is the neurotransmitter of a majority of amacrine cells (Wilson & Vaney, 2008), we suggest, therefore, that light-cytoplasm processes are likely from an amacrine cell, and may be GABAergic.

## Discussion

### Distribution of rEF terminals

In this study we show the distribution of rEF terminals in the chicken retina by mapping the position of every one. Our maps extend the qualitative observation from other studies of chicken retina (Catsicas *et al.*, 1987b; Fritzsch *et al.*, 1990; Morgan *et al.*, 1994; Fischer & Stell, 1999; Cellerino *et al.*, 2000) that rEF terminals are concentrated in the inferior retina. Exclusion from the superior retina is strict: of the 15,359 rEF terminals we counted in 2 retinas, only two errant terminals were present in the dorsal retina. Terminals of rEFs are also reportedly absent from the dorsal region of the quail retina (Uchiyama & Stell, 2005), but only in pigeon retina is a quantitative map available for comparison with our data (Hayes & Holden, 1983). Based on sampling of HRP filled efferent fibers in the retina, the pigeon retina map is similar to chicken in showing an absence of rEF terminals from the dorsal retina, but different in several other regards. Maximum density of terminals is somewhat higher in pigeon, 500 as opposed to 350/$mm^2$ but, like chicken, the maximum density is found close to the horizontal meridian. Unlike the chicken though, the distribution in pigeon is biased towards the temporal retina and the rEF terminal distribution extends higher in the retina than it does in chicken. Very likely these differences are correlated with differences in the visual fields of the two species and their typical eye position relative to the visual world.

Although this has received some attention in pigeon (see Nalbach *et al.*, 1993), a comparison is not possible as similar studies have not been done in chicken.

### rEFs give rise to three distinct types of synaptic terminal

The main synaptic connection of rEFs in the chicken retina is with target cells, known also as association amacrine cells (Fritzsch *et al.*, 1990; Uchiyama & Stell, 2005). These cells are readily recognized, unusually large, strongly parvalbumin-positive neurons. Every one of these neurons has a single rEF contacting it with multiple large boutons resembling a bunch of grapes. This main synaptic structure is somewhat different from either the pigeon or the quail. In the pigeon not all rEFs make contact with TCs, but those that do converge upon a TC soma with a few large boutons (Dowling & Cowan, 1966; Hayes & Holden, 1983). The description of the synapse in Dowling and Cowan (1966) and the one micrograph illustrating it, suggest that the complex dendritic basketwork we see in chicken might be absent from pigeon. In the quail, rEFs apparently end in single very large boutons that invaginate the basal part of the TC soma (Uchiyama & Ito, 1993).

The fact that in double labeled preparations we saw no TCs without rEF contacts confirms the supposition that TCs have no other function than as an element in the CVS. The one to one nature of the contact between rEFs and TCs is striking. Even though many rEFs split into branches while crossing the IPL, these branches nevertheless converge upon a single target cell. In this regard chicken differs from pigeon where a significant fraction of rEF branches diverge to separate targets (Dogiel, 1895; Maturana & Frenk, 1965; Hayes & Holden, 1983). We cannot rule out the possibility that, in the chicken, some small degree of branching of rEFs occurs in the optic nerve but this seems unlikely since in pigeon the number of rEFs in the retina closes matches the number of neurons in the ION(Hayes & Holden, 1983), and the same is probably true in chicken.

As in pigeon and quail (Dowling & Cowan, 1966; Uchiyama & Ito, 1993), the large presynaptic boutons of rEFs are loaded with vesicles, and as we show here, each bouton has multiple active zones apposed to either the TC soma or its diminutive dendrites. Together with other indications, such as myelination of rEFs (Cowan, 1970), this suggests that efferent input to target cells is both fast and very powerful. Almost certainly this is the largest synaptic structure between one neuron and another in the avian retina.

In addition to this major synaptic output, there are 2 other kinds of synaptic structure made by rEFs. A majority of rEF terminals give rise to a few fine processes (tendrils) that terminate in single small boutons at the bottom of the INL. In most cases we were unable to identify the postsynaptic partners of tendrils; however, we do know that in some cases tendril synaptic boutons apparently contacted the soma of a lightly diaphorase-positive amacrine cell, clearly the Type 1 cell described by Fischer and Stell (1999). Other authors have mentioned observing small side branches from rEF terminals (Ramón y Cajal, 1889; Maturana & Frenk, 1965; Chmielewski *et al.*, 1988; Fritzsch *et al.*, 1990); however, these side branches were not described in sufficient detail to allow comparison with the tendrils described here. Maturana and Frenk (1965) claimed that displaced ganglion cells were one of the synaptic partners of tendrils, but this claim has been contested in multiple studies (Dowling & Cowan, 1966; Fritzsch *et al.*, 1990; Uchiyama & Ito, 1993; Nickla *et al.*, 1994) and synapses between tendrils and DGCs were not observed here.

In addition to tendrils, we found that a minority of rEFs gave rise to a novel and unique, putatively synaptic structure that we have called the ball and chain. The most striking feature of this structure is the large (~5 μm diameter) terminal ball that is intensely diaphorase-positive, suggesting that the ball and chain is a significant source of nitric oxide (NO) in the retina. We were unable to identify the postsynaptic partner of this structure but it was not a

TC, nor any other kind of diaphorase-positive neuron. Considering the high diffusibility of NO (Dawson & Snyder, 1994), the cells influenced by this structure could be numerous. Alternatively, given evidence that mechanisms exist in the retina to limit the diffusion of NO to specific synaptic regions (Blute *et al.*, 2000), the postsynaptic targets could be limited to just those cells in physical contact with the ball.

### Synaptic interaction between rEFs and TCs occurs in a private neuropil

Lucifer yellow fills of target cells, EM studies, and diaphorase staining provide complementary and consistent pictures of the main synaptic output of rEFs. The number of presynaptic grapes varies by a factor of 5 and their placement is also variable. In all TCs, grapes were seen in a distinct neuropil region lying below the main part of the soma. In some TCs, grapes were pressed into the soma, forming what Cajal called a pericellular nest. The neuropil itself is a complex basketwork of stubby and anastomosing TC dendrites interwoven with the rEF terminals and processes contributed from other neurons. Significantly, this zone of synaptic contact does not lie within the IPL, where virtually all the synapses of other inner retina neurons are confined, but is restricted to a region of the INL between the base of the TC and the INL-IPL border, effectively forming a private neuropil.

While a superficially analogous situation occurs in the outer retina, where the pedicles of cones enclose a specialized region of synaptic contacts, a more illuminating parallel might be drawn with the glomeruli of the cat LGN. Here, as in the private neuropil of the TC, NO is thought to be a modulator (Sherman & Guillery, 2002), though of unknown function. Both the TC private neuropil, and the LGN glomerulus consist of a synaptic region segregated from surrounding neurons by a glial sheath and we might speculate that this plays a role in limiting the diffusion of NO.

### TCs receive synaptic input from putative retinal neuron terminals

The prevailing view of TCs is that they are “slave neurons” driven by efferent input (Uchiyama *et al.*, 2004). This is plausible in view of the massive input they receive from rEFs and the one to one nature of this contact. Within the private neuropil of the TC however, we show there are synaptic inputs to TCs from other neurons that we tentatively suggest may be GABAergic amacrine cells. The importance of these retinal inputs needs to be established through physiological recordings but, at a minimum, this suggests that local activity in the ventral retina can modify the responses of TCs.

### Implications for the Function of the CVS

An unusual and surprising feature of the CVS is that the axons of TCs project mostly to the dorsal retina but do so in a disorderly way (Catsicas *et al.*, 1987a; Uchiyama *et al.*, 2004) quite unlike the precise mapping found elsewhere in the CVS, as exemplified by the orderly retinotopic map found in the ION (Holden & Powell, 1972). The current interpretation of this anomaly is that, because TCs act merely as slave neurons, the placement of their somata is not tightly regulated and actually has no bearing on the functional topology of their wiring (Uchiyama *et al.*, 2004; Uchiyama & Stell, 2005). From this perspective, it is only the position of the TC axon terminal in the dorsal retina that is important and this, physiological data argues (Li *et al.*, 1998), is arranged to overlap the receptive field of the EF from which that TC receives input. Three findings we report here bear on to this interpretation. First, we find that rEF terminals and TCs are not just more concentrated within the ventral retina but are, in fact, strictly confined there. This might suggest that TC placement is tightly regulated rather than haphazard. Second, we find that TCs receive synaptic input from neurons in the ventral retina. The nature of this input can only be known through physiological recording but, like all neuronal signals in the retina, it must carry spatially specific information. Our

third finding is that rEFs, which we know from studies in pigeon (Holden & Powell, 1972; Miles, 1972), do themselves carry spatially specific information, make minor synapses with neurons other than TCs. In particular, a small field amacrine cell is one likely post synaptic partner. Taken together, these three observations argue that efferent terminal and TC position within the retina may be significant and in some way contribute to the function of the centrifugal visual system.

## Acknowledgments

We thank Leah Krubitzer and her lab for teaching us survival surgery, and Nathan Hart for help with some of the NADPH diaphorase experiments. This work was supported by NIH awards EY04112 and EY12576. Work was conducted in a facility constructed with support from Research Facilities Improvement Program Grant Number C06 RR-12088-01 from the National Center for Research Resources, National Institutes of Health.

## Literature Cited

Adams JC. Heavy metal intensification of DAB-based HRP reaction product. J Histochem Cytochem. 1981; 29:775. [PubMed: 7252134]

Blute TA, Lee MR, Eldred WD. Direct imaging of NMDA-stimulated nitric oxide production in the retina. Vis Neurosci. 2000; 17:557–566. [PubMed: 11016575]

Catsicas S, Catsicas M, Clarke PG. Long-distance intraretinal connections in birds. Nature. 1987a; 326:186–187. [PubMed: 3821893]

Catsicas S, Thanos S, Clarke PG. Major role for neuronal death during brain development: refinement of topographical connections. Proc Natl Acad Sci U S A. 1987b; 84:8165–8168. [PubMed: 3479784]

Cellerino A, Novelli E, Galli-Resta L. Retinal ganglion cells with NADPH-diaphorase activity in the chick form a regular mosaic with a strong dorsoventral asymmetry that can be modelled by a minimal spacing rule. Eur J Neurosci. 2000; 12:613–620. [PubMed: 10712641]

Chmielewski CE, Dorado ME, Quesada A, Geniz-Galvez JM, Prada FA. Centrifugal fibers in the chick retina. A morphological study. Anat Histol Embryol. 1988; 17:319–327. [PubMed: 3223603]

Cowan WM. centrifugal fibres of the avian retina. Br med Bull. 1970; 26:112–118.

Cowan WM, Powell TP. Centrifugal fibres to the retina in the pigeon. Nature. 1962; 194:487. [PubMed: 13881866]

Crossland WJ, Hughes CP. Observations on the afferent and efferent connections of the avian isthmo-optic nucleus. Brain Res. 1978; 145:239–256. [PubMed: 638787]

Dacey DM, Peterson BB, Robinson FR, Gamlin PD. Fireworks in the primate retina: in vitro photodynamics reveals diverse LGN-projecting ganglion cell types. Neuron. 2003; 37:15–27. [PubMed: 12526769]

Dawson TM, Snyder SH. Gases as biological messengers: nitric oxide and carbon monoxide in the brain. J Neurosci. 1994; 14:5147–5159. [PubMed: 8083727]

Dogiel AS. Die Retina der Vogel. Arch Mikrosk Anat. 1895; 44:622–648.

Dowling JE, Cowan WM. An electron microscope study of normal and degenerating centrifugal fiber terminals in the pigeon retina. Z Zellforsch Mikrosk Anat. 1966; 71:14–28. [PubMed: 5990091]

Fischer AJ, Stell WK. Nitric oxide synthase-containing cells in the retina, pigmented epithelium, choroid, and sclera of the chick eye. J Comp Neurol. 1999; 405:1–14. [PubMed: 10022192]

Fritzsch B, Crapon de Caprona MD, Clarke PG. Development of two morphological types of retinopetal fibers in chick embryos, as shown by the diffusion along axons of a carbocyanine dye in the fixed retina. J Comp Neurol. 1990; 300:405–421. [PubMed: 2266193]

Goureau O, Regnier-Ricard F, Jonet L, Jeanny JC, Courtois Y, Chany-Fournier F. Developmental expression of nitric oxide synthase isoform I and III in chick retina. J Neurosci Res. 1997; 50:104–113. [PubMed: 9379486]

Hayes BP, Holden AL. The distribution of centrifugal terminals in the pigeon retina. Exp Brain Res. 1983; 49:189–197. [PubMed: 6832256]

Hayes BP, Webster KE. Neurones situated outside the isthmo-optic nucleus and projecting to the eye in adult birds. Neurosci Lett. 1981; 26:107–112. [PubMed: 6272166]

Holden AL, Powell TP. The functional organization of the isthmo-optic nucleus in the pigeon. J Physiol. 1972; 223:419–447. [PubMed: 5039282]

Hoshino K, Hicks TP, Hirano S, Norita M. Ultrastructural organization of transmitters in the cat lateralis medialis-suprageniculate nucleus of the thalamus: an immunohistochemical study. J Comp Neurol. 2000; 419:257–270. [PubMed: 10723003]

Iliakis B, Anderson NL, Irish PS, Henry MA, Westrum LE. Electron microscopy of immunoreactivity patterns for glutamate and gamma-aminobutyric acid in synaptic glomeruli of the feline spinal trigeminal nucleus (Subnucleus Caudalis). J Comp Neurol. 1996; 366:465–477. [PubMed: 8907359]

Li JL, Xiao Q, Fu YX, Wang SR. Centrifugal innervation modulates visual activity of tectal cells in pigeons. Vis Neurosci. 1998; 15:411–415. [PubMed: 9685194]

Maturana HR, Frenk S. Synaptic connections of the centrifugal fibers in the pigeon retina. Science. 1965; 150:359–361. [PubMed: 5833792]

McGill JI, Powell TP, Cowan WM. The retinal representation upon the optic tectum and isthmo-optic nucleus in the pigeon. J Anat. 1966; 100:5–33. [PubMed: 5914538]

Miles FA. Centrifugal control of the avian retina. 2 Receptive field properties of cells in the isthmo-optic nucleus. Brain Res. 1972; 48:93–113. [PubMed: 4645218]

Mize RR, Whitworth RH, Nunes-Cardozo B, van der Want J. Ultrastructural organization of GABA in the rabbit superior colliculus revealed by quantitative postembedding immunocytochemistry. J Comp Neurol. 1994; 341:273–287. [PubMed: 8163727]

Montero VM, Singer W. Ultrastructure and synaptic relations of neural elements containing glutamic acid decarboxylase (GAD) in the perigeniculate nucleus of the cat. A light and electron microscopic immunocytochemical study. Exp Brain Res. 1984; 56:115–125. [PubMed: 6381084]

Morgan IG, Miethke P, Li ZK. Is nitric oxide a transmitter of the centrifugal projection to the avian retina? Neurosci Lett. 1994; 168:5–7. [PubMed: 7913217]

Nalbach, HO.; Wolf-Oberhollenzer, F.; Remy, M. Exploring the image. In: Zeigler, HP.; Bischof, H-J., editors. Vision, brain, and behavior in birds. MIT Press; Cambridge, Mass: 1993. p. 25-46.

Nickla DL, Gottlieb MD, Marin G, Rojas X, Britto LR, Wallman J. The retinal targets of centrifugal neurons and the retinal neurons projecting to the accessory optic system. Vis Neurosci. 1994; 11:401–409. [PubMed: 7516180]

Oberdorfer MD, Parakkal MH, Altschuler RA, Wenthold RJ. Ultrastructural localization of GABA-immunoreactive terminals in the anteroventral cochlear nucleus of the guinea pig. Hear Res. 1988; 33:229–238. [PubMed: 2898468]

Posada A, Clarke PG. Role of nitric oxide in a fast retrograde signal during development. Brain Res Dev Brain Res. 1999; 114:37–42.

Ramón y Cajal S. Sur la morphologie et les connexions des elements de la retine des oiseaux. Anatomischer Anzeiger. 1889; 4:111–121.

Ramón y Cajal S. Sobre unos corpusculos especiales de la retina de las aves. Actas de la Sociedad Espanola de Historia Natural. 1895; 24:128–130.

Ramón y Cajal, S. Histology of the nervous system of man and vertebrates. Oxford University Press; New York: 1995.

Rios H, Lopez-Costa JJ, Fosser NS, Brusco A, Saavedra JP. Development of nitric oxide neurons in the chick embryo retina. Brain Res Dev Brain Res. 2000; 120:17–25.

Sagar SM. NADPH diaphorase histochemistry in the rabbit retina. Brain Res. 1986; 373:153–158. [PubMed: 3719304]

Sanna PP, Keyser KT, Deerink TJ, Ellisman MH, Karten HJ, Bloom FE. Distribution and ontogeny of parvalbumin immunoreactivity in the chicken retina. Neuroscience. 1992; 47:745–751. [PubMed: 1584416]

Sherman SM, Guillery RW. The role of the thalamus in the flow of information to the cortex. Philos Trans R Soc Lond B Biol Sci. 2002; 357:1695–1708. [PubMed: 12626004]

Uchiyama H, Aoki K, Yonezawa S, Arimura F. Retinal target cells of the centrifugal projection from the isthmo-optic nucleus. J Comp Neurol. 2004; 476:146–153. [PubMed: 15248195]

Uchiyama H, Ito H. Target cells for the isthmo-optic fibers in the retina of the Japanese quail. Neurosci Lett. 1993; 154:35–38. [PubMed: 8361645]

Uchiyama H, Ito H, Tauchi M. Retinal neurones specific for centrifugal modulation of vision. Neuroreport. 1995; 6:889–892. [PubMed: 7612877]

Uchiyama H, Nakamura S, Imazono T. Long-range competition among the neurons projecting centrifugally to the quail retina. Vis Neurosci. 1998; 15:417–423. [PubMed: 9685195]

Uchiyama H, Stell WK. Association amacrine cells of Ramon y Cajal: rediscovery and reinterpretation. Vis Neurosci. 2005; 22:881–891. [PubMed: 16469195]

Vaney DI. Type 1 nitrergic (ND1) cells of the rabbit retina: comparison with other axon-bearing amacrine cells. J Comp Neurol. 2004; 474:149–171. [PubMed: 15156584]

Vaney DI, Young HM. GABA-like immunoreactivity in NADPH-diaphorase amacrine cells of the rabbit retina. Brain Res. 1988; 474:380–385. [PubMed: 3208139]

Vugler AA, Semo M, Joseph A, Jeffery G. Survival and remodeling of melanopsin cells during retinal dystrophy. Visual neuroscience. 2008; 25:125–138. [PubMed: 18442436]

Wilson, M.; Vaney, DI. Amacrine Cells In The Senses: A Comprehensive Reference. Academic Press; 2008. p. 361-368.

Woodson W, Shimizu T, Wild JM, Schimke J, Cox K, Karten HJ. Centrifugal projections upon the retina: an anterograde tracing study in the pigeon (Columba livia). J Comp Neurol. 1995; 362:489–509. [PubMed: 8636463]

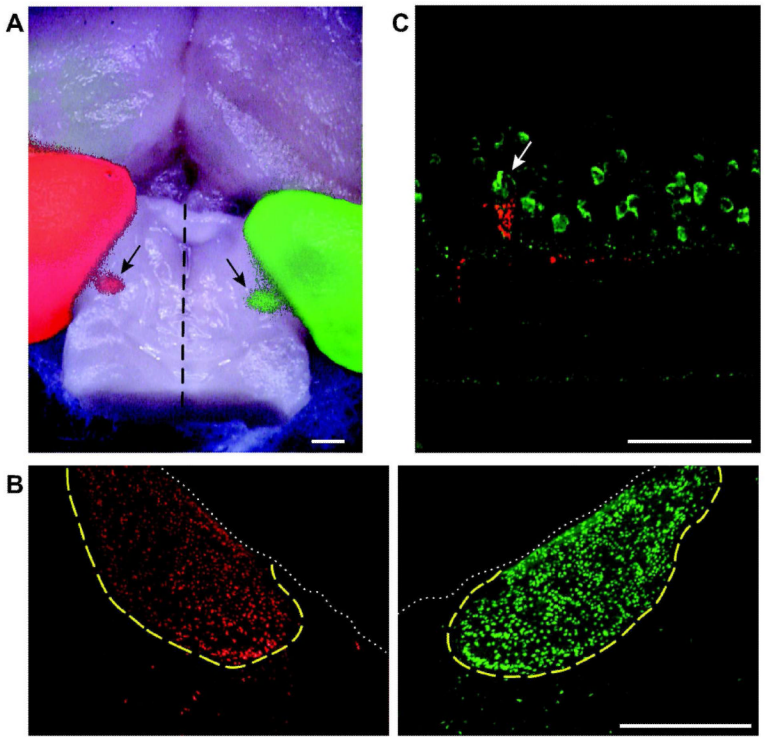


**Figure 1. Labeling of efferent fibers**

**A:** Dorsal surface of a chicken brain with fluorescent staining resulting from the injection of red and green Alexa-conjugated cholera toxin subunit B (CTB) into the right and left eyes, respectively. The cerebral hemispheres are visible in the upper half of the image, and the midbrain has been exposed by removing the cerebellum. The left (red) and right (green) optic tecta are visible on the left and right margins of the image. Between the two tecta, on the dorsal surface of the midbrain are two ovoid structures measuring approximately 1 mm across (arrows). These are the left (red) and right (green) IONs, located roughly 2 mm from the midline (dashed line). Anterior is up. Scale Bar is 1 mm. **B:** Transverse sections of the brain shown in **A**, cut through the midbrain showing left and right IONs. The dotted white line delineates the dorsal surface of the midbrain and the boundaries of the IONs are traced in yellow. The few CTB labeled neurons seen outside this boundary are the “ectopic neurons” that give rise to the widespread efferent fibers (wEFs). Dorsal is up. Scale Bar is 500 μm. **C:** Transverse section of the retina showing Fluoro-Ruby labeling of an rEF terminal (red). Multiple cells in the amacrine cell layer are parvalbumin + (green) but the TC around which the efferent terminal forms, can be distinguished by its larger size and prolate soma (arrow). Scale Bar is 50 μm.

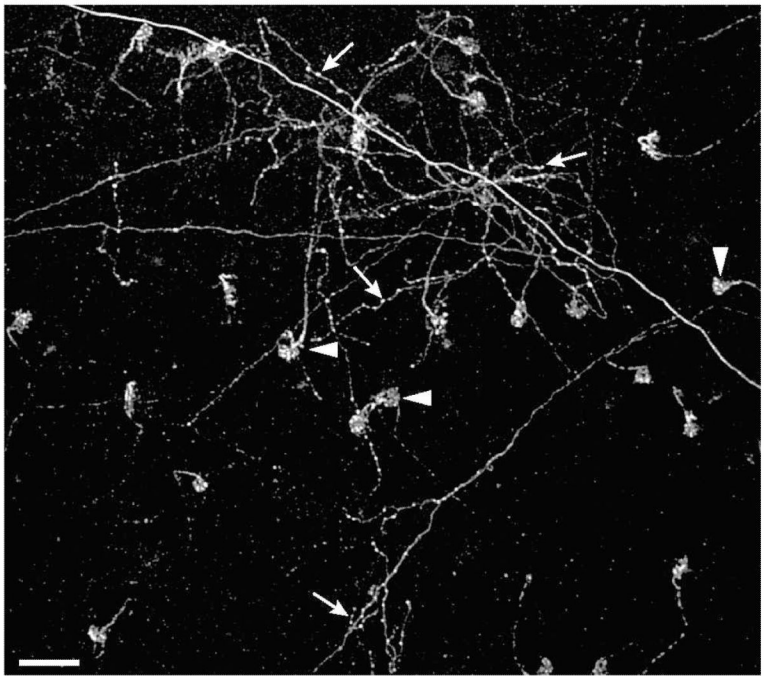

**Figure 2. Comparison of wEFs and rEFs**

Fluoro-Ruby labeled terminals shown at the border of the INL and IPL in the retina. The distinctive pericellular nests (arrowheads) can be seen as the terminals of 23 rEFs. In addition, the diffuse arborization of one or more wEFs (arrows) is shown. Unlike the rEFs, wEFs give rise to collaterals and have multiple swellings (likely synaptic boutons) throughout their axonal arborization. Scale Bar is 50 μm.

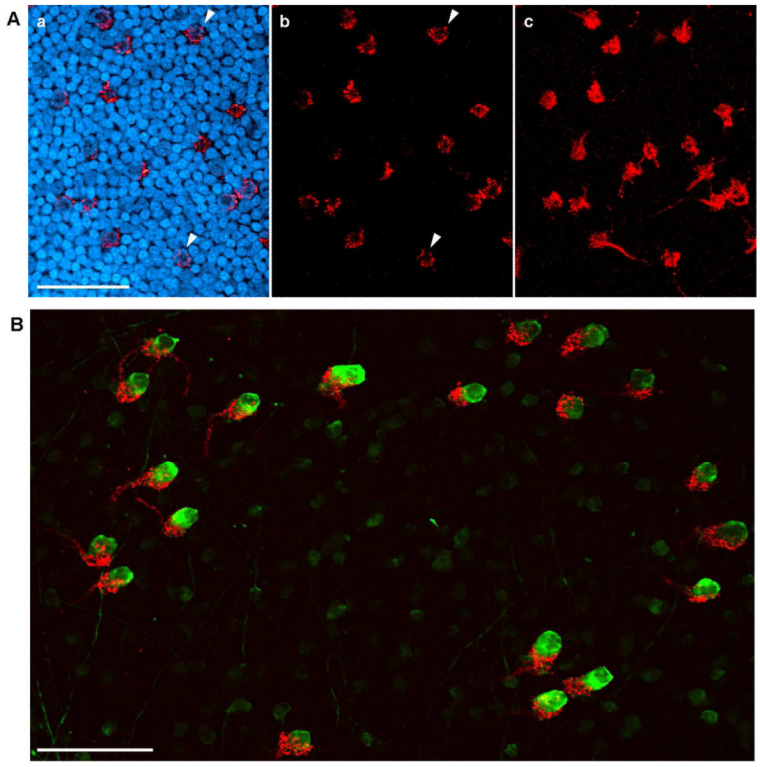


**Figure 3. Gross Structure of the rEF-TC Synapse**

**A:** A single confocal plane just below the equator of TC somata is shown in **a** and **b.** In **a,** INL somata are shown stained with SYBR-green (blue) but in **b** these are omitted. In this plane of the retina, the pericellular nest (red) wraps around the soma of the TC, giving the rEF terminal a donut shaped appearance (arrowheads). Panel **c** shows a collapsed z-stack of the entire pericellular nest. Scale Bar is 50 μm. **B:** A collapsed z-stack image from a retinal flat mount showing Fluoro-Ruby labeled rEFs (red) and parvalbumin immunofluorescence (green). TCs are clearly distinguishable from the other parvalbumin positive amacrine cells based on their larger size and more intense staining. Every TC is postsynaptic to a pericellular nest formed by a single rEF. Scale Bar is 50 μm.

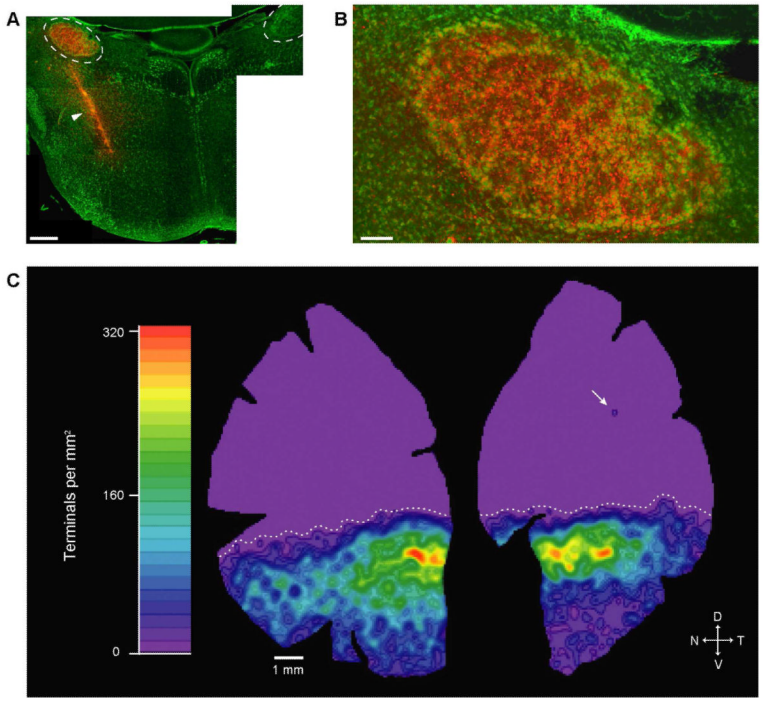


**Figure 4. Distribution and Density of rEF Terminals**

**A:** Montaged image of a transverse section from the midbrain of a chicken following stereotaxic injection of Fluoro-Ruby into the left midbrain. IONs are outlined with dashed lines. While the injection site (arrowhead) was medial and ventral to the ION, the injection path ran through the left ION resulting in labeling of the IO-neurons (compare with the unlabeled right ION). SYBR-green shows somata (green). Scale Bar is 500 μm. **B:** The left ION has been completely labeled by this injection, with every IO-neuron appearing yellow; thus all rEF terminals in the retina should be labeled. Scale bar is 100 μm **C:** Density map derived from the positions of all 7,193 rEF terminals in this retina. rEF terminals are found in highest density in a band below the horizontal midline, reaching a maximum of 320/mm$^2$ (red). Lower densities of rEFs were found throughout the ventral retina (green to blue). The dorsal retina is a uniform lavender, indicating that, with the exception of a single terminal in the upper temporal retina (arrow), rEFs are absent from this region. The transition from the high rEF density band to the dorsal region is abrupt (max. to 0 in 1.5 mm) creating a clear boundary between the ventral and dorsal retina (dotted line).

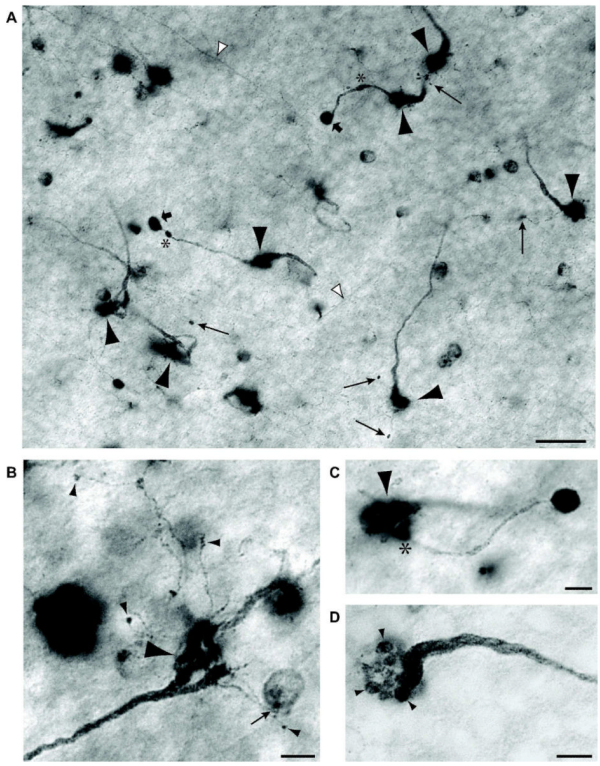


**Figure 5. NADPH-diaphorase staining of rEF terminals**

**A:** NADPH-diaphorase stained flat mount viewed at the INL/IPL boundary. Several rEF fibers give rise to large pericellular nests slightly out of the plane of focus (large arrowheads). Long arrows designate tiny boutons terminating fine “tendrils” arising from the pericellular nest. Another type of secondary synaptic structure, the “ball and chain” comprises a relative thick process, often with swellings (asterisks) terminating in a dense ball (broad arrows). The somata of other diaphorase-positive amacrine cells and target cell axons (white arrowheads) can also be seen in this image. Scale Bar is 20 μm. **B:** A high magnification image of a single rEF terminal to show the structure of tendrils in greater detail. Tendrils can be seen to branch off the pericellular nest (large arrowhead). These very slender branches terminate in small synaptic boutons on unknown targets in the amacrine cell layer (small arrowheads). One bouton contacts a weakly diaphorase positive amacrine cell (small arrow). Scale Bar is 5 μm. **C:** A high magnification image of a single rEF terminal to show the structure of a ball and chain in greater detail. A single chain (diameter 1-2 μm) branches off (*) the pericellular nest (arrowhead) and terminates in a large (approx. 5 μm) intensely NADPH-diaphorase positive ball. Scale Bar is 5 μm. **D:** A pericellular nest at high magnification is seen to comprise about 15, 2 μm diameter, presynaptic structures (arrowheads), giving it the appearance of a bunch of grapes at the end of the swollen efferent fiber. Scale Bar is 5 μm.

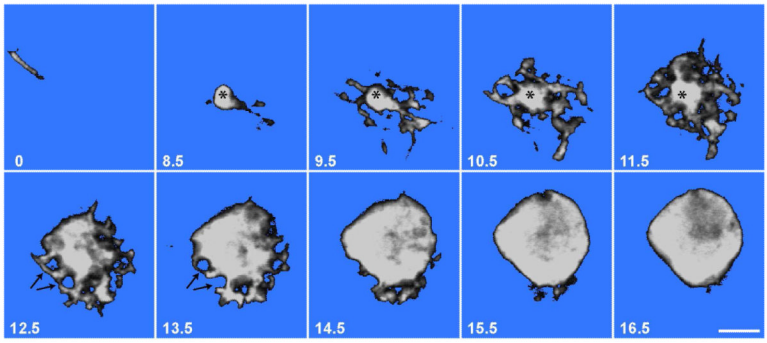


**Figure 6. Lucifer Yellow Filled TC**

A series of confocal z-sections showing a single Lucifer yellow-filled TC. The number in the lower left corner of each image represents distance from the INL-IPL border in μm. The upper left image (0 μm), shows the TC axon running parallel to the INL-IPL border. The axon initial segment (*) can be seen in images 8.5-11.5 μm where it gives rise to an intricate but tightly confined basketwork of dendrites. The basal region of the TC soma, 12.5-15.5 μm, shows 2 μm diameter holes (arrows) representing spaces filled by presynaptic grapes of the rEF. The TC soma equator lies at approximately 16.5 μm. Scale Bar is 5 μm.

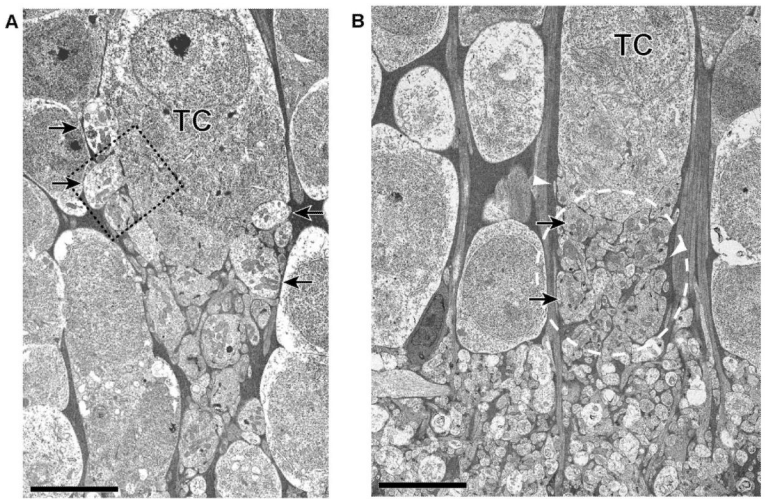


**Figure 7. Ultrastructure of TC**

Two TCs are shown here to illustrate the variability in synaptic organization. **A:** As with all TCs, this example shows a neuropil region below the soma but within the INL. Presynaptic grapes are visible in the neuropil region but are also pressed into the soma (arrows) approximately up to the equator of the soma. **B:** Presynaptic grapes (arrows), in this example are basal to the soma. The neuropil region (indicated by a dashed oval) lies above the IPL/INL boundary and is curtained off from the surrounding amacrine cells by a sheath of Muller cell processes (the electron dense areas indicated by white arrowheads). Scale Bar is 5 μm.

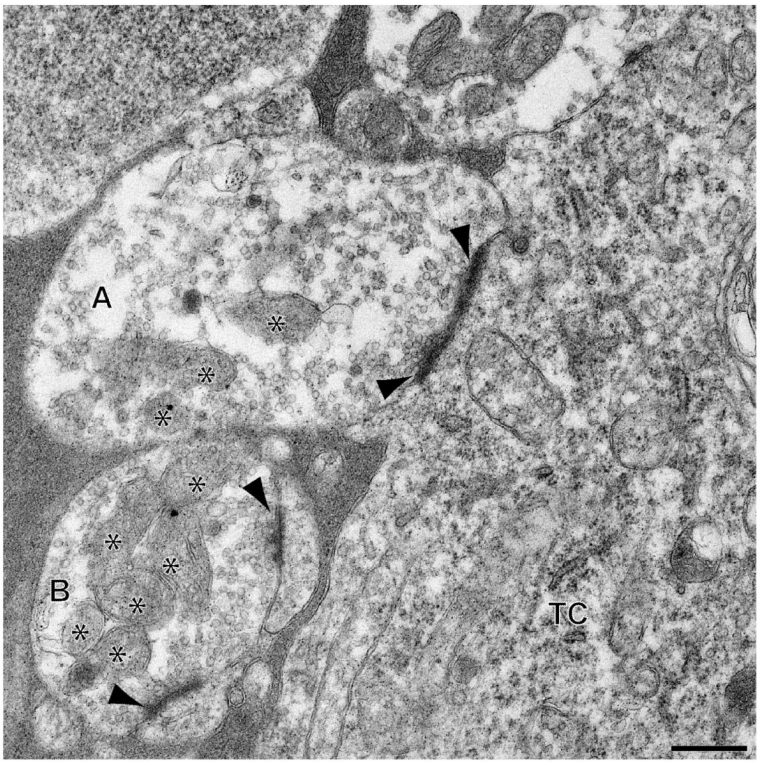


**Figure 8. Ultrastructure of rEF Presynaptic Boutons**

Two rEF presynaptic boutons (grapes) and a portion of the efferent target cell soma (TC) taken from the boxed region of Fig. 7A and shown at greater magnification. Cytoplasm of the TC is characterized by an abundance of ribosomes and rough endoplasmic reticulum. The larger rEF grape (**A**) is presynaptic to the TC soma and, in this plane, shows two active zones (arrowheads) around which are aggregations of clear, round synaptic vesicles. The smaller rEF grape (**B**) shows 2 synaptic densities (arrowheads) at which two small processes are the postsynaptic elements. Both grapes contain an abundance of mitochondria (asterisks). Scale Bar is 0.5 μm.

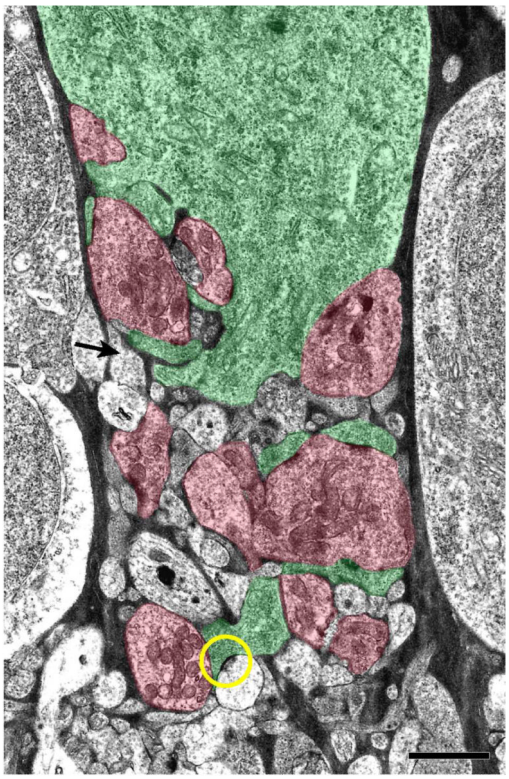

**Figure 9. Organization of the TC's Private Neuropil**

**A:** Using the cytoplasmic characteristics of the TC and rEF grapes, processes were identified and colored green or red, respectively. Processes that could not be unambiguously identified have been left uncolored. Some of these processes likely belong to the TC or rEF, but others are different, having very light cytoplasm and a low density of small, pleomorphic synaptic vesicles (arrow shows one example). A second process of this type is seen presynaptic to one of the TC dendrites (yellow circle). Scale Bar is 2 μm.